

# Modification of Polystyrene by Reactive Extrusion with Peroxide and Trimethylolpropane Triacrylate

Byung Kyu Kim,<sup>1</sup> Kyung Ho Shon,<sup>1</sup> Han Mo Jeong<sup>2</sup>

<sup>1</sup>Department of Polymer Science and Engineering, Pusan National University, Pusan 609–735, Republic of Korea

<sup>2</sup>Department of Chemistry and Research Center for Machine Parts and Materials Processing, University of Ulsan, Ulsan 680–749, Republic of Korea

Received 8 January 2003; accepted 7 October 2003

**ABSTRACT:** Polystyrene (PS) was modified by reactive extrusion with trimethylolpropane triacrylate (TMPTA) and dicumyl peroxide (DCP). The coupling reaction caused by TMPTA increased the molecular weight of PS, and this coupling reaction was enhanced in the presence of DCP at high TMPTA/DCP ratio. The rheological properties of the extrudate were examined. The impact strength of PS im-

proved as the molecular weight increased by the coupling reaction. © 2004 Wiley Periodicals, Inc. *J Appl Polym Sci* 92: 1672–1679, 2004

**Key words:** polystyrene; reactive extrusion; trimethylolpropane triacrylate; molecular weight; viscoelastic properties

## INTRODUCTION

Reactive extrusion, using free radical chemistry, was found to be an effective and economical way of achieving postreactor modification of polymers.<sup>1–11</sup> Appreciable improvements in the physical and chemical properties and the processability of polymers or polymer blends can be achieved via chain scission, long chain branching, crosslinking, and grafting. Depending upon the polymer system and the specific processing conditions, these mechanisms may occur simultaneously or one of them may be dominant. For example, polyethylene (PE) and polypropylene (PP) respond to the attack of a peroxide free radical in opposite ways. PP undergoes mostly chain scission, whereas PE crosslinks.<sup>12–16</sup> However, the efficiency of the crosslinking reaction of both PE and PP can be enhanced by the addition of coagents (crosslinking activators) such as trimethylolpropane triacrylate (TMPTA), pentaerythritol triacrylate, and triallyl isocyanurate.<sup>17,18</sup> These are typically reactive multifunctional monomers and many of them are from the class of methacrylates or allyl compounds.

The tension stiffening response of polymer melt is required in the process with extensional flow such as foaming, vacuum forming, blowing, or coating for stable manufacturing. The tension stiffening can be

enhanced by long chain branching or by the presence of a small concentration of high molecular weight species.<sup>19–22</sup> So, the coupling reaction by reactive extrusion was effectively utilized to enhance the tension stiffening of polymer melt.

In the case of polystyrene (PS), it was reported that organic peroxides enhance chain scission rather than crosslinking.<sup>23,24</sup> Although this chain scission can be reduced by some chemicals such as maleic anhydride,<sup>25</sup> to the best knowledge of the present authors no paper has reported on the peroxide initiated reactive extrusion of PS where the crosslinking or coupling reaction was dominant. In this study we tried to obtain the reactive extrusion conditions where the coupling reaction was dominant over chain scission, and rheological and mechanical properties of the extrudates were examined.

## EXPERIMENTAL

The PS used in this experiment was polymerized thermally in the absence of initiator and has average molecular weight  $M_w = 180,000$ ,  $z$  average molecular weight,  $M_z = 390,000$ , melt volume index (MVI, 200°C, 5 kg) = 7.5 cm<sup>3</sup>/10 min. The viscosity number in Table I is the reduced viscosity obtained by dividing the specific viscosity by the concentration (grams per milliliter) of polymer in toluene solution and was determined according to DIN 53,726 at 25°C.

Dicumyl peroxide (DCP, Hansol Chemical) and TMPTA (Junsei) were used as received without further purification.

Reactive extrusion was carried out with a corotating twin-screw extruder (Berstorff ZE25, L/D = 33.5) at a

Correspondence to: H. M. Jeong (hmjeong@mail.ulsan.ac.kr).

Contract grant sponsor: University of Ulsan Research Fund of 2002.

TABLE I  
Molecular Characteristics of Extruded PS

Sample no.	Additive		Molecular characteristics				
	DCP (phr)	TMPTA (phr)	MVI (cm <sup>3</sup> /10 min)	Viscosity No. (mL/g)	$M_w$	$M_z$	$M_z/M_w$
1	—	—	9.3	78.0	172,100	362,900	2.1
2	0.025	—	9.6	76.6	170,100	356,500	2.1
3	0.025	1.00	7.2	80.2	261,900	1,728,000	6.6
4	0.025	1.50	5.6	83.6	354,800	2,732,100	7.7
5	0.050	—	11.9	73.4	163,500	331,900	2.0
6	0.050	1.00	7.0	81.3	305,800	2,279,500	7.5
7	0.050	2.00	5.1	85.1	416,100	3,387,600	8.1
8	—	1.00	9.2	78.2	182,200	391,200	2.1
9	—	1.50	7.2	79.8	186,500	422,300	2.3
10	—	2.00	6.8	80.2	191,600	485,800	2.5

zone temperature profile of 190–210°C and 250 rpm. Extrudates were quenched in water and pelletized. After being dried at 80°C for 2 h, the extrudate was injection molded with a Arburg 221-75-350 injection machine. The machine was set at a barrel temperature profile of 200–210°C and a mold temperature of 50°C. PS pellet, DCP, and TMPTA were mixed thoroughly before extrusion. During the reactive extrusion, minute amounts of volatile products were formed, and these were removed in the degassing zone of the extruder, where a vent hole is provided.

Molecular weight was evaluated at 30°C with gel permeation chromatography (GPC, Waters M510) equipped with a set of six Waters Ultrastaygel columns (100, 500, 10<sup>3</sup>, 10<sup>4</sup>, 10<sup>5</sup>, and 10<sup>6</sup> Å). Tetrahydrofuran was used as an eluant.

Melt rheological properties shown in Figures 2–7 were measured with a parallel plate fixture of an Advanced Rheometrics Expansion System (Rheometrics). The measurements were carried out isothermally at 200, 220, and 240°C. The test fixtures were preheated to the measured temperature, samples were subsequently charged, and the excess material was

trimmed followed by conditioning for several minutes to relax the residual stress. The frequency sweep was done with 15% strain, which is the upper limit where the linear viscoelastic behavior was maintained. All of the experiments were carried out in a nitrogen environment to avoid oxidative degradation.

The 3.2-mm unnotched Izod impact strength, tensile properties of the injection molded specimen, and MVI were determined according to the standard procedure described in ASTM D256, D638, and D1238, respectively. The dumbbell-shape tensile specimen had dimensions of 57.0 mm length, 13.0 mm width, and 3.2 mm thickness. The specimens were elongated at the rate of 50 mm/min. MVI was measured at 200°C with 5 kg load.

## RESULTS AND DISCUSSION

### Molecular characteristics

When we compare the molecular characteristics of Sample 1 in Table I with those of virgin PS before extrusion (see Experimental), we see that thermal deg-

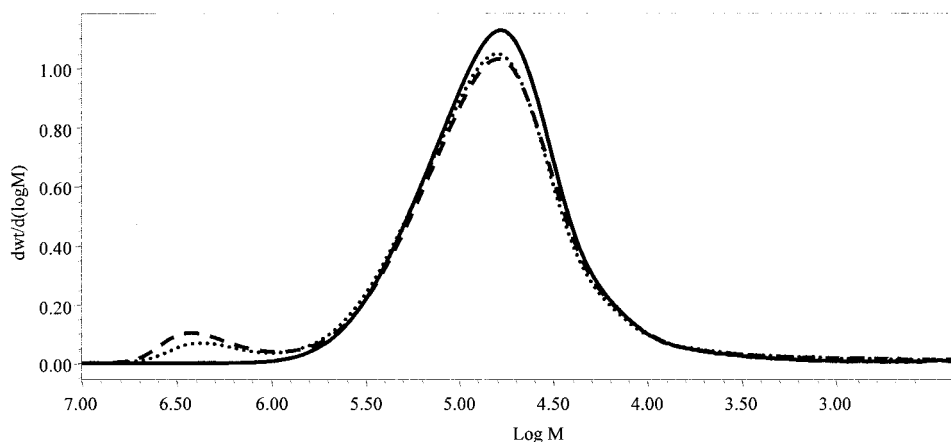
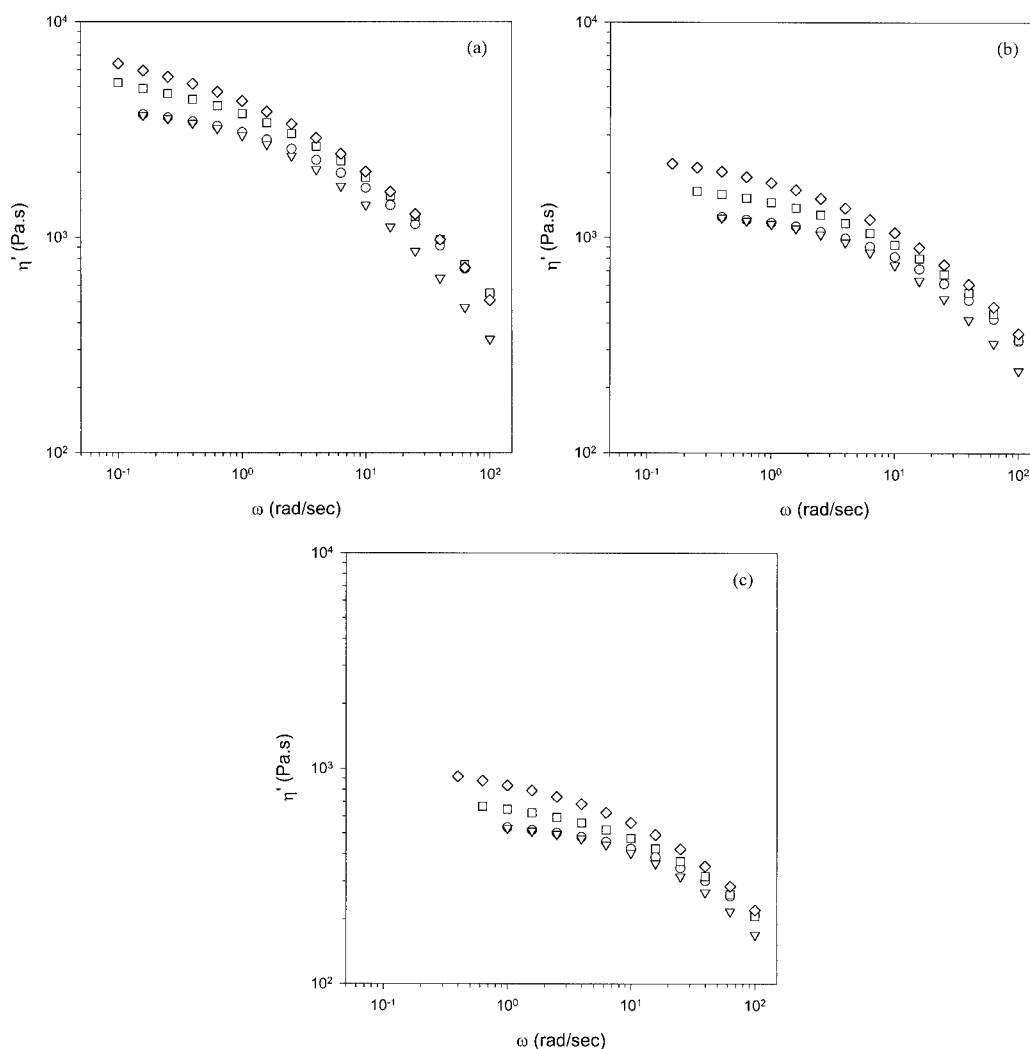


Figure 1 Molecular weight ( $M$ ) distributions of (—) Samples 1, (···)6, and (- -) 7.



**Figure 2** Dynamic viscosity versus shear rate of (○) Samples 1, (∇) 5, (□) 6, and (◇) 7 measured at (a) 200°C, (b) 220°C, and (c) 240°C.

radation occurs even in the absence of DCP or TMPTA. This thermal degradation of PS during melt processing was reported to be initiated mainly by the generation of free radical by the thermal cleavage of weak links, such as head-to-head linkage, initiator fragments, unsaturation, branch points, and peroxide groups.<sup>23,25,26</sup>

When we compare the molecular characteristics of Samples 1, 2, and 5 in Table I, we see that this degradation reaction is promoted in the presence of DCP because free radical generated from DCP can abstract hydrogen from the PS backbone and  $\beta$ -scission of the PS backbone occurs from this PS radical.<sup>23</sup>

The molecular characteristics of Samples 8–10 in Table I show that the molecular weight of PS increases as the concentration of TMPTA increases.<sup>17</sup> This result shows that the coupling between PS-TMPTA-PS can occur in the absence of peroxide.<sup>27</sup>

The results of Samples 3 and 4 and 6 and 7 show that the coupling reaction by TMPTA is enhanced in

the presence of DCP at high TMPTA/DCP feed ratio. In Figure 1 we see that a shoulder due to high molecular weight species is evident by the effective coupling reaction at high TMPTA/DCP feed ratio.

### Rheological properties

Figures 2 and 3 present the dynamic viscosities of PS modified with TMPTA and DCP. As expected, the dynamic viscosity increases as the molecular weight increases by the coupling reaction with TMPTA and DCP.

At very low frequencies, the oscillatory deformation can be considered nearly a steady state flow, and the very general phenomenological theory of Coleman and Markovitz<sup>28</sup> predicts a simple relationship (Eq. 1) between the two viscosities,

$$\lim_{\omega \rightarrow 0} \eta'(\omega) = \lim_{\dot{\gamma} \rightarrow 0} \eta(\dot{\gamma}), \quad (1)$$

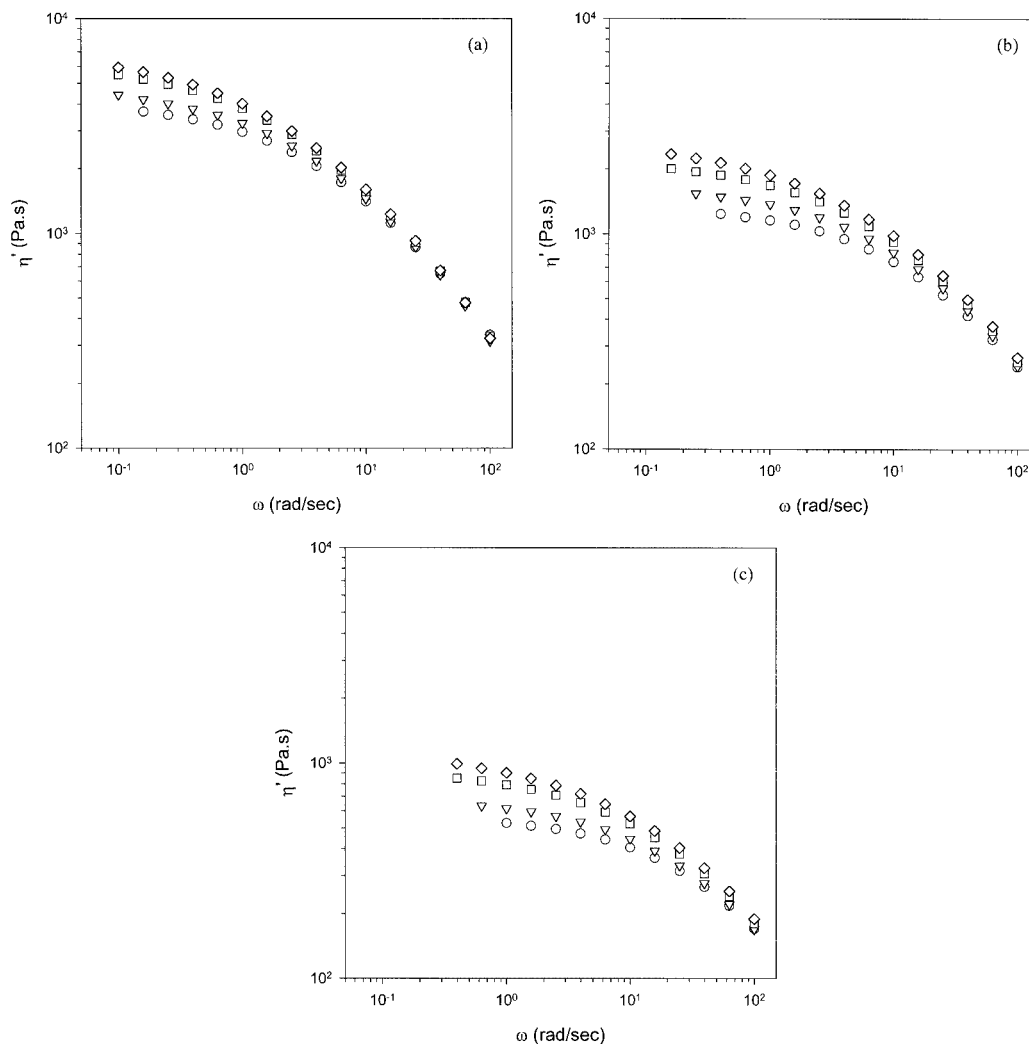


**Figure 3** Dynamic viscosity versus shear rate of (○) Samples 1, (▽) 8, (□) 9, and (◇) 10 measured at (a) 200°C, (b) 220°C, and (c) 240°C.

where  $\eta'$  is dynamic viscosity, that is, the in-phase component of complex viscosity,  $\eta$  is steady flow viscosity,  $\omega$  is the frequency in rad/s, and  $\dot{\gamma}$  is steady shear rate. The zero-shear steady flow viscosity,  $\eta_0$ ,

**TABLE II**  
Zero-Shear Steady Flow Viscosities of Extruded PS

Sample No.	Zero-shear steady flow viscosity (Pa · s)		
	200°C	220°C	240°C
1	4020	1330	560
2	3860	1190	480
3	5320	1710	680
4	6120	2080	860
5	3490	1090	440
6	5500	1740	710
7	6690	2350	980
8	4650	1630	670
9	6000	2140	910
10	6550	2550	1080

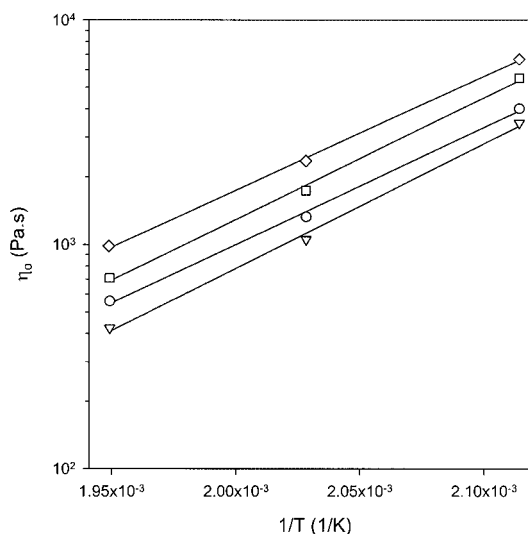


**Figure 4**  $\eta_0$  versus  $1/T$  of (○) Samples 1, (▽) 5, (□) 6, and (◇) 7.

**TABLE III**  
**Activation Energy for Flow Process of Extruded PS**

Sample No.	Activation energy (J/mol)
1	99,200
2	104,900
3	103,600
4	98,800
5	104,200
6	103,300
7	96,700
8	97,600
9	95,000
10	90,900

can be determined from low shear data using Ferry's equation (Eq. 2)<sup>29</sup>,

$$1/\eta = 1/\eta_0 + b\tau, \tag{2}$$

where  $b$  is a constant and  $\tau$  is the shear stress corresponding to  $\eta$ . Such plots gave reasonably good straight lines, and the results are given in Table II. It is known that  $\log \eta_0$  is proportional to some average molecular weight which is between  $M_w$  and  $M_z$ .<sup>30</sup> In Table II we can see that  $\eta_0$  generally increases with some exceptions as  $M_w$  and  $M_z$  are increased by coupling reaction.

The dependence of  $\eta_0$  on temperature was calculated from the Arrhenius equation (Eq. 3),

$$\eta_0 = Ae^{(E/RT)}, \tag{3}$$

where  $E$  is the activation energy for flow process,  $R$  is the gas constant,  $T$  is the absolute temperature (K), and  $A$  is a constant. The results for Samples 1 and 5-7 are shown in Figure 4 and the values of activation energies are given in Table III. In the series of Samples 2-4, 5-7, and 8-10, activation energy generally de-

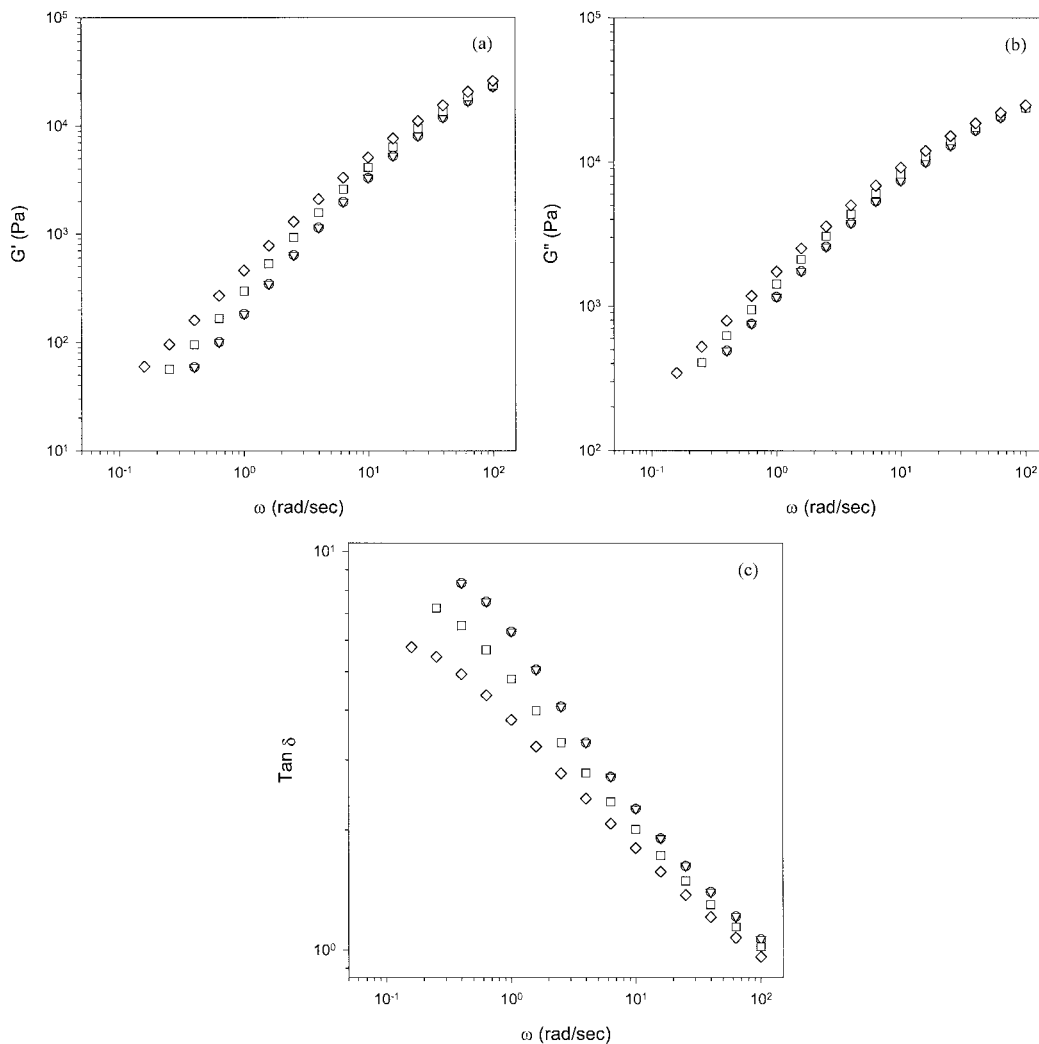


**Figure 5** (a) Storage modulus  $G'$ , (b) loss modulus  $G''$ , and (c) ratio of loss modulus over storage modulus,  $\tan \delta$  versus shear rate of (○) Samples 1, (▽) 5, (□) 6, and (◇) 7 measured at 220°C.

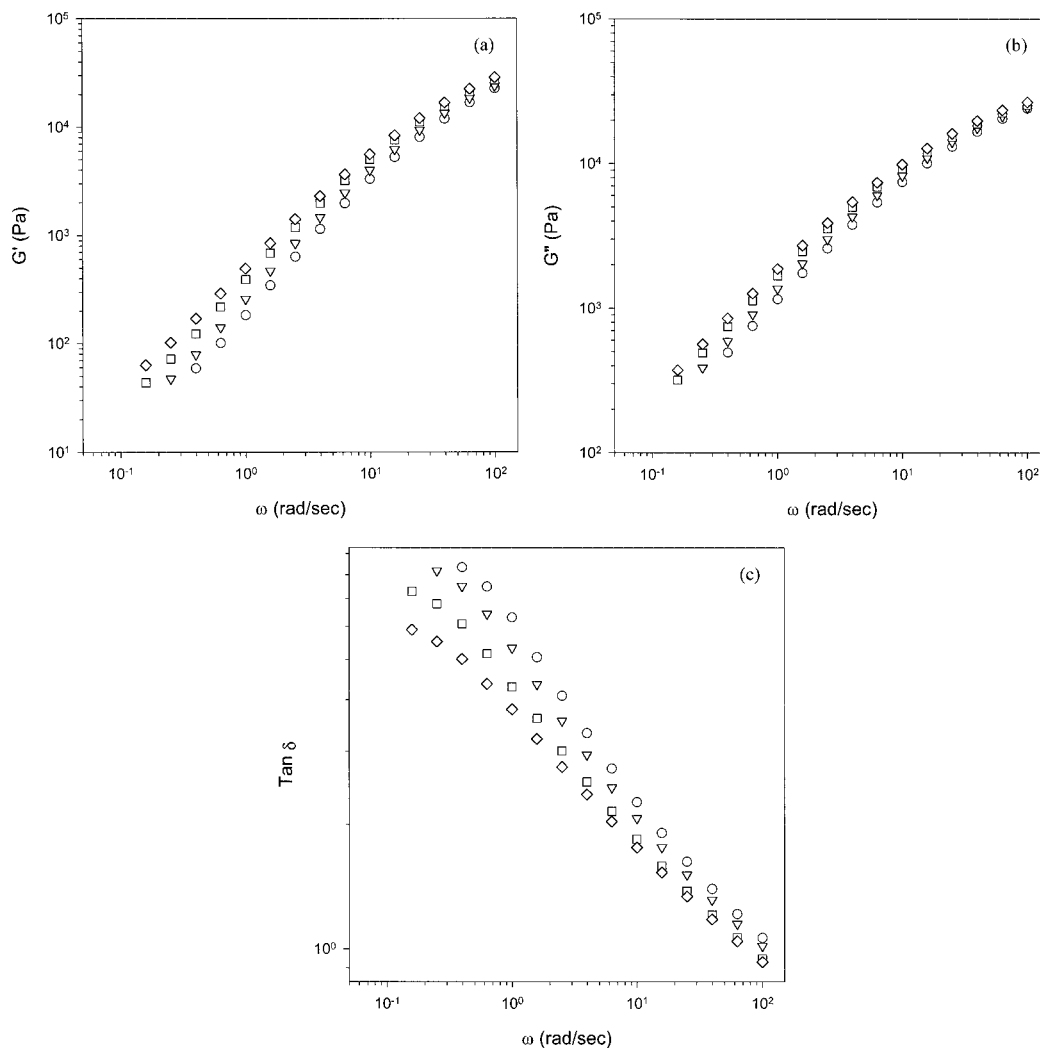


**Figure 6** (a) Storage modulus  $G'$ , (b) loss modulus  $G''$ , and (c) ratio of loss modulus over storage modulus,  $\tan \delta$  versus shear rate of (○) Samples 1, (▽) 8, (□) 9, and (◇) 10 measured at 220°C.

creases as the molecular weight is increased by the coupling reaction. This shows that the dependence of  $\eta_0$  on temperature is reduced by the coupling reaction.

**TABLE IV**  
Crossover Frequency and Crossover Modulus of Extruded PS at 200°C

Sample No.	$\omega_c$ (rad/s)	$G_c$ (Pa)
1	39.7	$2.57 \times 10^4$
2	44.2	$2.65 \times 10^4$
3	32.1	$2.48 \times 10^4$
4	27.8	$2.38 \times 10^4$
5	50.2	$2.79 \times 10^4$
6	31.9	$2.49 \times 10^4$
7	26.1	$2.31 \times 10^4$
8	33.7	$2.41 \times 10^4$
9	25.7	$2.30 \times 10^4$
10	24.5	$2.30 \times 10^4$

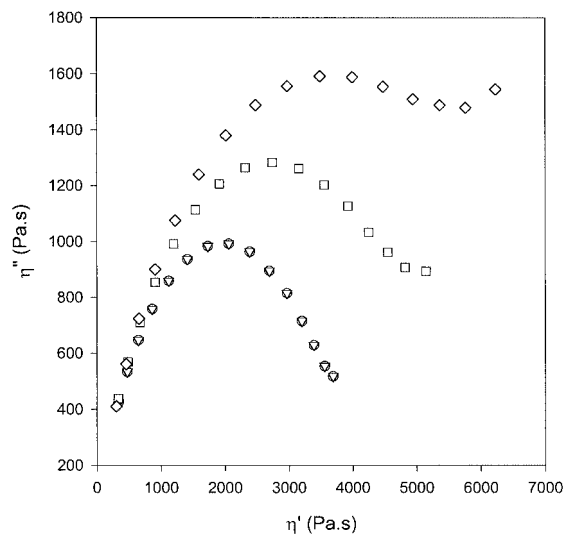


**Figure 7** Cole-Cole plots at 200°C of (○) Samples 1, (▽) 5, (□) 6, and (◇) 7.

TABLE V  
Mechanical Properties of Extruded PS

Sample No.	Unnotched Izod impact strength (kg <sub>f</sub> · cm/cm)	Yield strength (kg <sub>f</sub> /cm <sup>2</sup> )	Tensile properties	
			Tensile strength at break (kg <sub>f</sub> /cm <sup>2</sup> )	Elongation at break (%)
1	11.9	477	477	2.0
2	11.0	430	430	2.0
3	12.0	450	450	2.0
4	13.0	450	450	2.0
5	10.5	419	419	2.0
6	13.6	450	450	2.0
7	14.2	445	445	2.0
8	11.9	466	466	2.0
9	12.5	461	461	2.0
10	12.8	457	457	2.0

Figures 5 and 6 show the variation of storage modulus,  $G'$ , and loss modulus,  $G''$ , as the frequency increases, where we can see that both  $G'$  and  $G''$  generally increase at low frequency as the molecular weight is increased by the coupling reaction. In the dynamic response of a linear amorphous polymer, samples of different molecular weight and molecular weight distribution merge at high frequency since the response depends only on the local chain motion.<sup>31</sup> The  $G'$  at low shear rate increases rapidly to plateau value when the molecular weight is increased, and  $G''$  at low shear rate increases as the high molecular weight fraction is increased.<sup>32</sup> This explains the results of Figures 5 and 6.

In Figures 5 and 6, we see that  $G''/G'$ , i.e.,  $\tan \delta$  values at low shear rate, generally decrease as the molecular weight is increased by the coupling reaction. This suggests that elastic deformation, compared with viscous flow with energy dissipation, is enhanced after the coupling reaction by increased chain entanglements.

The crossover point, the point at which  $G' = G''$ , has interesting and useful properties. It was reported that the frequency at the crossover point,  $\omega_c$ , decreased as the molecular weight increased in narrow molecular weight distribution 1,4-polybutadiene samples.<sup>33</sup> The crossover modulus,  $G_c$ , was increased as the polydispersity was decreased.<sup>32</sup> The values of  $\omega_c$  and  $G_c$  are shown in Table IV, where we see that both  $\omega_c$  and  $G_c$  generally decrease as the molecular weight and  $M_z/M_w$  are increased by the coupling reaction in Samples 2–4, 5–7, and 8–10.

Figure 7 shows the Cole–Cole plots of PS samples measured at 200°C. The Cole–Cole plot of polymer having unimodal-type molecular weight distribution gives a semicircle.<sup>34</sup> However, the Cole–Cole plot of polymer with bimodal molecular weight distribution having two discrete relaxation time distributions drifts from semicircle.<sup>35</sup> In Figure 7, we see

that the Cole–Cole plot drifts from semicircle when the degree of the coupling reaction is high and the shoulder by high molecular weight fraction exists in Figure 1.

### Mechanical properties

In Table V, we see that impact strength is generally increased as the molecular weight is increased by the coupling reaction in Samples 2–4, 5–7, and 8–10. This shows that the increase of molecular weight by the coupling reaction is affirmative for the enhancement of impact strength. However, Table V shows that the effect of coupling reaction on tensile properties are rather minor or negative.

### CONCLUSION

We observed in this study that TMPTA could increase the molecular weight of PS by coupling reaction during reactive extrusion. This coupling reaction was enhanced in the presence of DCP at high TMPTA/DCP ratios, and GPC curves showed a shoulder of high molecular weight species generated by the coupling reaction. The enhanced entanglement of PS chains by the coupling reaction increased  $\eta_0$ , the activation energy for flow process, and impact strength.

### References

- Xanthos, X.; Dagli, S. S. *Polym Eng Sci* 1991, 31, 929.
- Vivier, T.; Xanthos, M. *J Appl Polym Sci* 1994, 54, 569.
- Bremner, T.; Rudin, A. *J Appl Polym Sci* 1995, 57, 271.
- Teh, J. W.; Rudin, A. *Polym Eng Sci* 1992, 32, 1678.
- Al-Malaika, S.; Artus, K. *J Appl Polym Sci* 1933 1998, 69.
- Mathew, A. P.; Packirisamy, S.; Thomas, S. *J Appl Polym Sci* 2000, 78, 2327.
- Crevecoeur, J. J.; Nelissen, L.; van der Sanden, M. C. M.; Lemstra, P. J.; Mencer, H. J.; Hogt, A. H. *Polymer* 1995, 36, 753.

8. Hu, G.-H.; Li, H.; Feng, L.-F.; Pessan, L. A. *J Appl Polym Sci* 2003, 88, 1799.
9. Graebing, D. *Macromolecules* 2002, 35, 4602.
10. Koster, M.; Hellmann, G. P. *Macromol Mater Eng* 2001, 286, 769.
11. Fukuoka, T. *Polym Eng Sci* 2000, 40, 2524.
12. Ebner, K.; White, J. L. *Intern Polymer Processing* 1994, IX, 233.
13. Ryu, S. H.; Gogos, C. G.; Xanthos, M. *Adv Polym Technol* 1992, 11, 121.
14. Triacca, V. J.; Gloor, P. E.; Zhu, S.; Hrymak, A. N.; Hamielec, A. E. *Polym Eng Sci* 1993, 33, 445.
15. Gaylord, N. G.; Mehta, M.; Mehta, R. *J Appl Polym Sci* 1987, 33, 2549.
16. Sajkiewicz, P.; Phillips, P. J. *J Polym Sci Polym Chem* 1995, 33, 853.
17. Kim, B. K.; Kim, K. J. *Adv Polym Technol* 1993, 13, 263.
18. Suyama, S.; Ishigaki, H.; Watanabe, Y.; Nakamura T. *Polym J* 1995, 27, 503.
19. Zhu, S. *Macromolecules* 1998, 31, 7519.
20. Tung, L. H.; Hu, A. T.; McKinley, S. V.; Paul, A. M. *J Polym Sci Polym Chem* 1981, 19, 2027.
21. Sugimoto, M.; Tanaka, T.; Masubuchi, Y.; Takimoto, J.; Koyama, K. *J Appl Polym Sci* 1999, 73, 1493.
22. Laun, H. M.; Schuch, H. *J Rheol* 1989, 33, 119.
23. Kim Y. C.; McCoy, B. J. *Ind Eng Chem Res* 2000, 39, 2811.
24. Smith W. B.; Temple, H. W. *J Phys Chem* 1968, 72, 4613.
25. Gaylord N. G.; Elayaperumal, P. *J Polym Sci Polym Lett* 1983, 21, 781.
26. Krstina, J.; Mcad, G.; Solomon, D. H. *Eur Polym J* 1989, 25, 767.
27. Teh, J. W.; Rudin, A. *Polym Eng Sci* 1991, 31, 1033.
28. Coleman, B. D.; Markovitz, H. *J Appl Phys* 1964, 35, 1.
29. Ferry, J. D. *Viscoelastic Properties of Polymers*, 2nd ed.; Wiley: New York, 1970.
30. Nielsen, L. E. *Polymer Rheology*; Dekker: New York, 1977.
31. Watanabe, H.; Sakamoto, T.; Kotaka, T. *Macromolecules* 1985, 18, 1008.
32. Rahalkar, R. R. *Rheol Acta* 1989, 28, 166.
33. Rahalkar, R. R. *Rheol Acta* 1990, 29, 88.
34. Marin, G.; Labaig, J. J.; Menge, Ph. *Polymer* 1975, 16, 223.
35. Han C. D.; Yang, H. H. *J Appl Polym Sci* 1987, 33, 1221.